

Optical properties of the charge-density-wave polychalcogenide compounds R_2Te_5 ($R=Nd, Sm$ and Gd)

F. Pfuner¹, L. Degiorgi^{1,a}, K.Y. Shin², and I.R. Fisher²

¹ Laboratorium für Festkörperphysik, ETH – Zürich, 8093 Zürich, Switzerland

² Geballe Laboratory for Advanced Materials and Department of Applied Physics, Stanford University, Stanford, California 94305-4045, USA

Received 13 December 2007 / Received in final form 14 April 2008

Published online 30 May 2008 – © EDP Sciences, Società Italiana di Fisica, Springer-Verlag 2008

Abstract. We investigate the rare-earth polychalcogenide R_2Te_5 ($R=Nd, Sm$ and Gd) charge-density-wave (CDW) compounds by optical reflectivity measurements. We obtain the optical conductivity through Kramers-Kronig transformation of the reflectivity spectra. From the real part of the optical conductivity we then extract the excitation energy of the CDW gap and estimate the fraction of the Fermi surface which is gapped by the formation of the CDW condensate. In analogy to previous findings on the related RTe_n ($n = 2$ and 3) families, we establish the progressive closing of the CDW gap and the moderate enhancement of the metallic component upon chemically compressing the lattice.

PACS. 71.45.Lr Charge-density-wave systems – 78.20.-e Optical properties of bulk materials and thin films

1 Introduction

The rare-earth polychalcogenides [1] RX_n (where R is the rare earth element, X denotes S, Se and Te, and $n = 2, 2.5, 3$) have recently attracted great interest due to their low dimensionality. Among the RX_n families are members that variously host large commensurate distortions, ordered and disordered vacancy structures, and (small-amplitude) Fermi surface driven charge-density-wave (CDW). Furthermore, the discovery of a pressure-induced superconductivity state in $CeTe_2$ [2] competing with a CDW phase and an antiferromagnetic order makes the rare-earth tellurides an ideal system to investigate the consequences that the interplay or competition between those phases has on fermionic excitations at the Fermi energy. In a broader perspective, they may help providing a deeper understanding of how superconductivity might result from such an interplay, an issue of great interest in the solid state community.

The CDW state has its origin in the well-known Peierls transition. Peierls first pointed out that a one-dimensional metal is unstable, when turning on the electron-phonon interaction, and undergoes a metal-insulator phase transition accompanied by a lattice distortion [3]. The new modulation of the lattice induces a periodic potential, which will be screened by the itinerant charge carriers

through the formation of the charge-density-wave condensate. Consequently, the opening of a (CDW) gap at the Fermi surface (FS) as well as the formation of a collective density wave state are the two most relevant fingerprints, characterizing a CDW broken symmetry ground state [4]. The CDW gap acts as an order parameter of the phase transition and its determination is of relevance in order to get more insight about the impact of the transition on the electronic properties and Fermi surface, as well.

Optical spectroscopic methods proved to be a powerful experimental tool and were widely used over the past few decades, in order to address the electrodynamic response in CDW materials [4]. Recently, we have thoroughly studied the optical properties of the RTe_2 and RTe_3 series [5–7]. They are closely related families, which are based on single (RTe_2) and double (RTe_3) Te-layers, separated by RTe block layers. We have discovered that the CDW gap is progressively reduced upon compressing the lattice in RTe_3 [5,6]. This is accompanied by a release of additional charge carriers into the conducting channel, leading to a moderate enhancement of the Drude term (i.e., plasma frequency) in the optical spectra. Nonetheless, for both $n = 2$ and $n = 3$ series our optical findings establish that a large fraction of the Fermi surface is gapped by the CDW formation [5,7].

In comparison to RTe_2 and RTe_3 , little is known about the R_2Te_5 family of compounds [8]. Their orthorhombic crystal structure ($Cmcm$) is intermediate between that of

^a e-mail: degiorgi@solid.phys.ethz.ch

$R\text{Te}_2$ and $R\text{Te}_3$, comprising alternating single and double Te (ac) planes sandwiched between $R\text{Te}$ corrugated block layers, stacked along the b axis. The existence of this class of compound raises the question of whether separate modulation wave vectors might exist on the single and double Te planes, respectively, and if so how these wave vectors might interact or compete with each other. The origin of the CDW has been argued in terms of the electron instabilities through the calculation of the Lindhard susceptibility, based on the LMTO band structure [8]. Recent transmission electron microscopy (TEM) investigations gave the first evidence for the CDW formation and established that the title compounds host a modulation wave vector, similar to that of the tri-telluride compounds. The critical temperature (T_{CDW}) for the CDW phase transition has not yet been identified, but is certainly well above 300 K [8], so that these materials are deep in the CDW state already at room temperature. In addition, each $R_2\text{Te}_5$ compound exhibits at least one further set of superlattice peaks. Consideration of the electronic structure led to the conclusion that independent wave vectors must be associated separately with sheets of the Fermi surface deriving from single and double Te layers, respectively [8]. One could also speculate that even the CDW gap may be different from one layer to the other, eventually manifesting in a broad mid-infrared absorption.

We present here our optical investigation on $R_2\text{Te}_5$, with $R=\text{Nd}$, Sm and Gd . The main goal is to shed light on their complete optical spectrum in order to extract the relevant energy scales, as the CDW gap and the Drude plasma frequency. In a broader context, we also wish to establish, in parallel to structural considerations, a comparison with the related rare-earth di- and tri-telluride families.

2 Experiment and results

We obtain the optical reflectivity $R(\omega)$ of all samples over a broad spectral range from the far-infrared up to the ultraviolet ($50\text{--}50000\text{ cm}^{-1}$ or $0.006\text{--}6\text{ eV}$). We have investigated the ac plane of our samples with unpolarized light, since the search for a polarization dependent optical response always failed, supporting the optical isotropic nature of the ac plane. The complete optical response is achieved by combining three different spectrometers: for the far- and mid-infrared region we make use of the Bruker Fourier-Transform interferometer IFS 113, equipped with a Bolometer detector, as well as a Bruker (IFS 48) spectrometer, while for the visible and ultraviolet range we employ the Perkin Elmer Lambda 950 spectrometer. Further details pertaining to the experiment can be found elsewhere [9,10].

The single crystals of the investigated compounds were grown by slow cooling a binary melt. Further details about their crystal growth and their characterization, particularly with respect to the CDW modulation vectors, can be found in reference [8]. As a consequence of a small exposed liquidus in the binary alloy phase diagram [11], crystals of $R_2\text{Te}_5$ grown by this technique often have a

thin layer of $R\text{Te}_3$ on their outermost surface. This layer can be removed by cleaving using sticky tape, and X-ray experiments have revealed that the remaining $R_2\text{Te}_5$ crystal is phase pure. From the optical point of view this issue is well illustrated in Figure 1a, which displays the spectra of Nd_2Te_5 as grown and after cleaving. The spectrum of the as-grown sample is indeed identical with the one of NdTe_3 . One cleaving action is enough to remove the spurious $R\text{Te}_3$ phase at the surface. Repeated cleaving procedures do not change the optical response anymore. Similar to $R\text{Te}_3$, crystals of $R_2\text{Te}_5$ are readily oxidized, and care was taken to avoid prolonged exposure to air when preparing the specimens for our optical investigations. We could hinder aging effects by storing the samples in a clean atmosphere (in the glove box or inside our cryostat).

The main panel of Figure 1b displays the $R(\omega)$ spectra for the cleaved surfaces of the three compounds at 300 K. It is worth noting that all cleaved surfaces were shiny and flat so that no specific correction procedures of the measured $R(\omega)$ spectra were necessary. Two features are clearly evident: the overall metallic behavior represented by the onset of increasing $R(\omega)$ below $4 \times 10^3\text{ cm}^{-1}$, and a broad absorption, peaked around 5000 cm^{-1} . This latter absorption leads to a more or less pronounced depletion in $R(\omega)$ (arrow in Fig. 1b), bearing striking similarities with previous data on $R\text{Te}_3$ [5] and $R\text{Te}_2$ [7]. In contrast to the metallic-like temperature dependence of the dc resistivity [12], we did not observe any significant temperature dependence of $R(\omega)$ in the measured energy interval. As an example, in the inset of Figure 1b we display $R(\omega)$ for Gd_2Te_5 below 10^4 cm^{-1} at 300 and 10 K. $R(\omega)$ in the far infrared range is at 10 K about 2–3% higher than at 300 K and both $R(\omega)$ signals progressively decrease and then merge with increasing frequencies so that they coincide at about 8000 cm^{-1} . The weak temperature dependence of $R(\omega)$ does not dramatically affect the optical properties (see below).

The real part $\sigma_1(\omega)$ of the complex optical conductivity is extracted from the Kramers-Kronig transformation of our reflectivity data [9,10]. To this end, the data were appropriately extended to zero frequency ($\omega \rightarrow 0$) with the Hagen-Rubens extrapolation ($R(\omega) = 1 - 2\sqrt{\frac{\omega}{\sigma_{dc}}}$) and at high wavenumbers with a power-law extrapolation ω^{-s} ($2 \leq s \leq 4$) [9,10]. The σ_{dc} values, inserted in the Hagen-Rubens formula, are in fair agreement with the dc transport data [12]. The resulting $\sigma_1(\omega)$ for each compound at 300 K is displayed in Figure 2, which emphasizes the features already pointed out in the reflectivity spectra (Fig. 1b). For all three compounds, $\sigma_1(\omega)$ is showing the so-called Drude peak in the low frequency range (with onset at frequencies $\omega \leq 1000\text{ cm}^{-1}$), associated to excitations due to the free charge carriers, and a broad peak in the energy interval between 2000 and 8000 cm^{-1} . Furthermore, $\sigma_1(\omega)$ displays other features at high frequencies ($\omega \geq 10000\text{ cm}^{-1}$), which can be tentatively ascribed to the onset of electronic interband transitions. Indeed, band structure calculations for the $R\text{Te}_n$ series [8,13] suggest electronic excitations at energies above 10^4 cm^{-1} . The inset of Figure 2 displays the resulting temperature

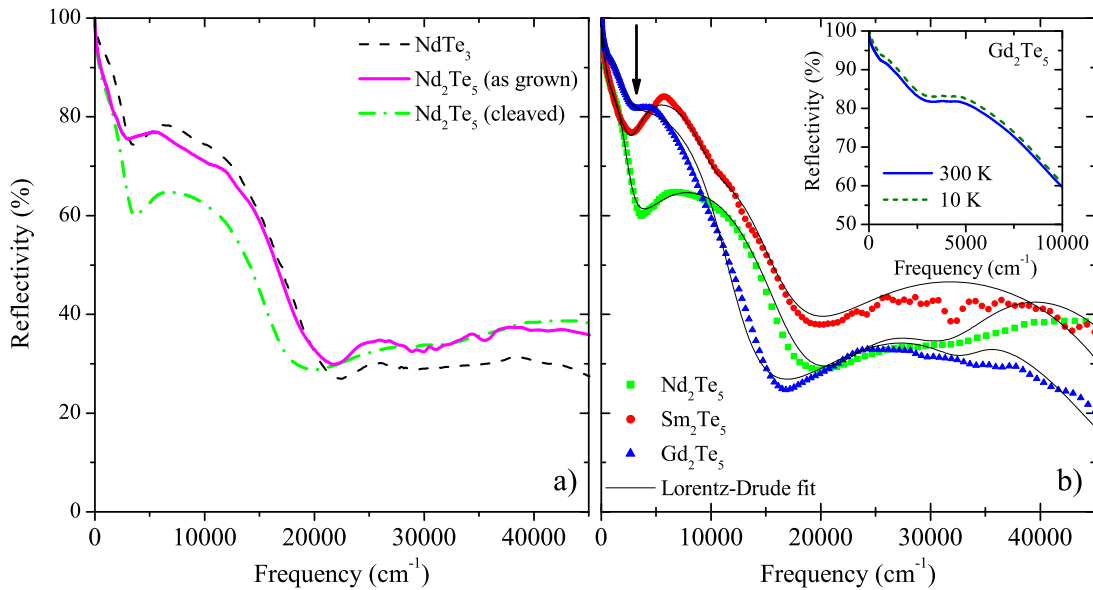


Fig. 1. (Color online) (a) Comparison of the Nd_2Te_5 spectra, for the as-grown sample as well as for the cleaved one, with the optical response of the related NdTe_3 compound [5]. (b) Optical reflectivity for the cleaved surfaces of $R_2\text{Te}_5$ with $R = \text{Nd}, \text{Sm}$ and Gd at 300 K. Thin lines are the Lorentz-Drude fit, as described in the main text. The fit parameters are summarized in Table 1. The arrow points out the depletion at about 4000 cm^{-1} . Inset: the weak temperature dependence of $R(\omega)$ in Gd_2Te_5 between 300 and 10 K is shown for frequencies below 10^4 cm^{-1} .

dependence of $\sigma_1(\omega)$ in the far infrared range, as obtained by the KK transformation of the spectra in the inset of Figure 1b. As anticipated above, because of the weak temperature dependence of $R(\omega)$ the optical conductivity starts to diverge between 300 and 10 K only when entering the far infrared spectral range.

For a detailed discussion of our results we apply the phenomenological Lorentz-Drude approach. It is a common tool to analyse the optical response in condensed matter and consists first of all in reproducing the complex dielectric function by the following expression [9,10]:

$$\tilde{\epsilon}(\omega) = \epsilon_1(\omega) + i\epsilon_2(\omega) = \epsilon_\infty - \frac{\omega_p^2}{\omega^2 + i\omega\gamma_D} + \sum_n \frac{S_n^2}{\omega_n^2 - \omega^2 - i\omega\gamma_n}. \quad (1)$$

ϵ_∞ is the optical dielectric constant, ω_p the plasma frequency and γ_D the scattering rate of the Drude term, whereas S_n^2 , ω_n and γ_n are the mode strength, the center frequency and the width of the n th Lorentz harmonic oscillator (h.o.), respectively. From equation (1) we can then calculate all optical properties (e.g., the real part $\sigma_1(\omega) = \omega \frac{\epsilon_2(\omega)}{4\pi}$ of the optical conductivity) as well as fully reproduce the measured $R(\omega)$ spectra. We systematically fit the optical spectra of the title compounds with four harmonic oscillators for the absorptions at finite frequencies, besides the Drude term for the metallic response. The fit components are shown in Figure 2 for all investigated materials, while the fit parameters at 300 K are summarized in Table 1. The results of the fit in both $R(\omega)$ and $\sigma_1(\omega)$ are shown in Figures 1b and 2, respectively, and tes-

tify a good agreement with the experiments. Because of the weak temperature dependence of our $R(\omega)$ spectra in the measured spectral range, all fit parameters turn out to be almost unchanged as a function of temperature. This is not surprising for those parameters associated with the high frequency CDW features (like, e.g., the broad mid-infrared excitation). However, it is somehow remarkable that the change of the scattering rate, as it would be expected from the dc transport properties, does not affect $\sigma_1(\omega)$ in the measured energy interval (inset Fig. 2). This seems to be a characteristic feature of this class of polychalcogenides [5,7]. As encountered in good metals, it is nevertheless reasonable to assume that the effects of reduced scattering with temperature manifest at very low energy scales, well beyond the far infrared.

3 Discussion

The depletion at about 4000 cm^{-1} in $R(\omega)$ (arrow in Fig. 1b) and the corresponding mid-infrared absorption between 2000 and 8000 cm^{-1} in $\sigma_1(\omega)$ are ascribed to the single particle peak (SP), due to the excitation across the CDW gap. This is in accordance with previous findings on related families; namely, $R\text{Te}_2$ and $R\text{Te}_3$ [5,7]. Angle resolved photoemission spectroscopy (ARPES) results for Gd_2Te_5 give evidence for an energy scale of about 500 meV (4000 cm^{-1}) for the CDW gap [14]. Common to other rare-earth tellurides, the SP feature is rather broad, particularly as far as its low frequency side is concerned. This may suggest a possible distribution of gaps on FS, as also recognized in $R\text{Te}_2$ and $R\text{Te}_3$ by ARPES data [15,16] and emphasized by our optical finding [5,7], as well. Similar to

Table 1. Rare-earth dependence in $R_2\text{Te}_5$ of the single particle peak ω_{SP} , the plasma frequency ω_p and the scattering rate γ_D of the Drude term, the resonance frequency ω_n , the damping Γ_n and the square root S_n of the mode strength of the n th Lorentz harmonic oscillators (all entries in 10^3 cm^{-1}), as well as of the optical dielectric constant ϵ_∞ and the ratio Φ .

	ω_{SP}	ω_p	γ_D	ω_1	Γ_1	S_1	ω_2	Γ_2	S_2	ω_3	Γ_3	S_3	ω_4	Γ_4	S_4	ϵ_∞	Φ
Nd_2Te_5	5.3	12	0.5	1.0	1.8	14	6.0	7.5	35	24	13	31	33	12	20	1.3	0.18
Sm_2Te_5	2.6	14	0.6	1.5	3.2	23	3.7	2.7	25	11	6.4	12	23	18	34	1.21	0.15
Gd_2Te_5	2.1	14	0.3	0.7	1.2	15	2.9	4.4	21	21	18	34	34	6.2	5.9	1.14	0.23

$R\text{Te}_2$ and $R\text{Te}_3$, the calculated FS for the unmodulated crystal structure of $R_2\text{Te}_5$ is imperfectly nested [17], such that one can anticipate a range of gap sizes around the FS in the CDW state. There are perfectly nested regions with a large gap and non-perfectly nested ones with small gap or even with no gap at all. For the $R_2\text{Te}_5$ compounds, there is additionally the issue of the distinctly different lattice modulations, which may live on different parts of the crystal structure (single and double Te layer). The wave vectors for the two modulations might have different temperature dependence. The consequent wealth of gaps, observed in our optical view of the Brillouin zone, tends to spread out over a large energy interval, even merging into the high frequency tail of the metallic contribution. Obviously, we are not able optically to say anything firm about the gap distribution beyond this phenomenological guess, since we are essentially integrating over the entire FS.

From a pure phenomenological point of view, the gap distribution or, more straightforward, the broad SP is fitted with two Lorentz h.o.'s in equation (1) [18], while the remaining two h.o.'s at high frequencies (i.e., $\omega \geq 10^4 \text{ cm}^{-1}$) mimic the absorptions due to the interband transitions (Fig. 2). In analogy to our previous analysis [5,7], it seems again convenient to introduce the so-called weighted energy scale ω_{SP} :

$$\omega_{SP} = \frac{\sum_{j=1}^2 \omega_j S_j^2}{\sum_{j=1}^2 S_j^2}, \quad (2)$$

where the sum extends over the first two h.o.'s of the mid infrared absorption. ω_{SP} represents the center of mass of the SP excitation and is summarized in Table 1. The optical findings on $R_2\text{Te}_5$ confirm the overall trend in both ω_{SP} and ω_p , already encountered in related rare-earth telluride families. Upon compressing the lattice there is a diminishing impact of the CDW phase, which is reflected in the decrease of ω_{SP} as well as in the moderate enhancement of ω_p . Progressively closing the gap also means that additional free charge carriers are released into the conduction channel, thus increasing the weight of the Drude term. Figure 3a displays the energy scale ω_{SP} as a function of the in-plane lattice constant a for the rare-earth telluride $R\text{Te}_n$ ($n = 2, 2.5$ and 3) series. It is quite appreciable that all these compounds are characterized by a common reduction of the CDW gap upon compressing the lattice. Moreover, it is worth recalling that the progressive suppression of the CDW gap upon compressing the lattice

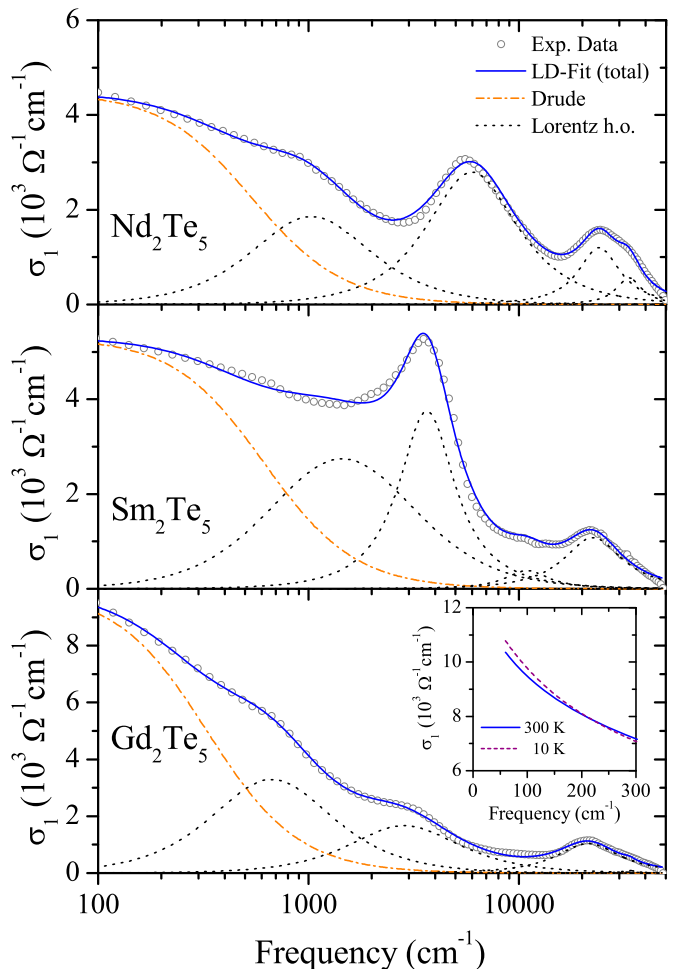


Fig. 2. (Color online) Real part $\sigma_1(\omega)$ of the complex optical conductivity for the three title compounds (logarithmic energy scale). The total Lorentz-Drude (LD) fit as well as its components are shown for each compound. All fit parameters are given in Table 1. The inset displays the far-infrared $\sigma_1(\omega)$ of the Gd-compound at 300 and 10 K.

has been recently discovered in the optical properties of CeTe_3 [6] and LaTe_2 [19] under externally applied pressure.

Sum rule arguments allow us to estimate the fraction of FS, affected by the formation of the CDW condensate. Following our previous work on NbSe_3 [20], $R\text{Te}_2$ [5] and

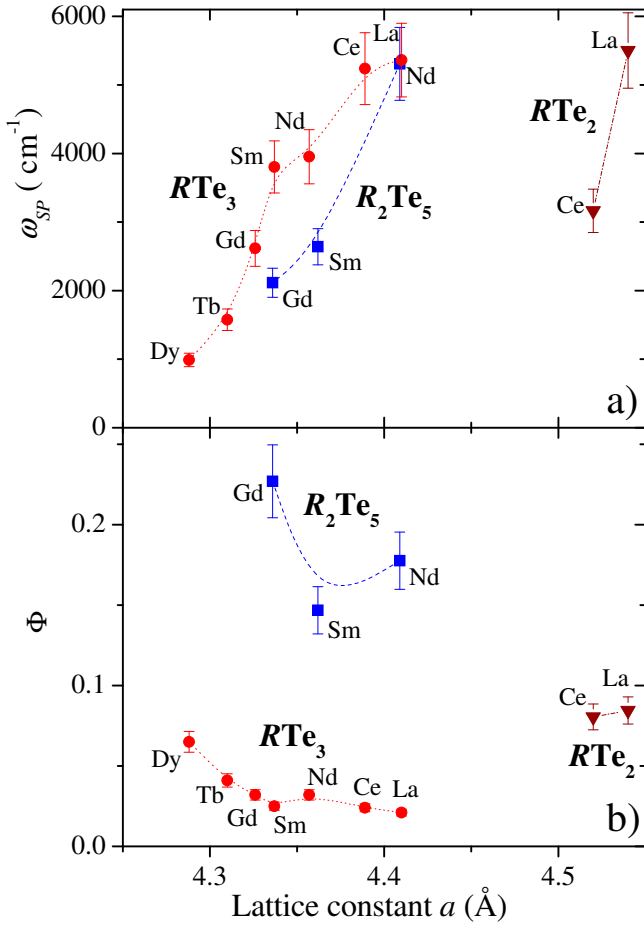


Fig. 3. (Color online) a) The single particle peak frequency ω_{SP} (Eq. (2)) and b) the ratio Φ (Eq. (3)) are shown as a function of the in-plane lattice constant a for the $R_2\text{Te}_5$, $R\text{Te}_3$ [5] and $R\text{Te}_2$ [7] series.

$R\text{Te}_3$ [7], we can define the ratio:

$$\Phi = \frac{\omega_p^2}{\omega_p^2 + \sum_{j=1}^2 S_j^2} \quad (3)$$

between the Drude weight in the CDW state and the total spectral weight of the hypothetical normal state. This latter quantity is achieved by assuming that above T_{CDW} the weight of the single particle peak (i.e., $\sum_{j=1}^2 S_j^2$) merges together with the Drude weight. Equation (3) provides a measure of how much of the FS survives in the CDW state. The values of Φ for $R_2\text{Te}_5$ are displayed in Table 1, while Figure 3b visualizes the comparison of the ratio Φ between the three families of compounds. The overall increase in Φ with chemical pressure for $R_2\text{Te}_5$ (i.e., of about 20% from the Nd to the Gd compound) follows a similar trend to that which is observed for $R\text{Te}_3$ [5], even though the fraction of the ungapped FS in the CDW state appears to be larger in $R_2\text{Te}_5$ than in other polychalcogenides (Fig. 3b). The non-monotonic behavior of Φ in $R_2\text{Te}_5$ could be ascribed to the variation in lattice modulations between the three compounds, in contrast to $R\text{Te}_3$ for which the lat-

tice modulation is the same. Sm_2Te_5 is in this regard quite peculiar among the $R_2\text{Te}_5$ materials, since it is characterized by two independent CDWs, commensurate along the in-plane c -axis and incommensurate along the in-plane a -axis. These CDWs are pertinent to the Te double and single layers, respectively [8]. It is believed furthermore that the two CDWs as well as the two types of Te layers interact more in the Sm compound than in the other two.

4 Conclusions

We provided here thorough optical investigations of the electrodynamic response of three representative members of the $R_2\text{Te}_5$ family of compounds, which share several common features with previous findings on related polychalcogenides. The CDW gap decreases upon compressing the lattice, thus generalizing concepts already developed for the $R\text{Te}_2$ and $R\text{Te}_3$ series. It is believed that the presence of single and double Te-layers in the crystal structure of $R_2\text{Te}_5$ [8] considerably affects the nesting properties of the Fermi surface as well as the impact of the CDW condensate on the electronic properties of these materials. In this context one might eventually explain the subtle differences among the title compounds as far as the FS gapping is concerned.

The authors wish to thank J. Müller for technical help, T. Müller for her contribution in the first stage of the data collection, and A. Sacchetti and M. Lavagnini for fruitful discussions. This work has been supported by the Swiss National Foundation for the Scientific Research within the NCCR MaNEP pool. This work is also supported by the Department of Energy, Office of Basic Energy Sciences under contract DE-AC02-76SF00515.

References

1. E. DiMasi, M.C. Aronson, J.F. Mansfield, B. Foran, S. Lee, Phys. Rev. B **52**, 14516 (1995)
2. M.H. Jung, A. Alsmadi, H.C. Kim, Y. Bang, K.H. Ahn, K. Umeo, A.H. Lacerda, H. Nakotte, H.C. Ri, T. Takabatake, Phys. Rev. B **67**, 212504 (2003)
3. R. Peierls, *Quantum Theory of Solids* (Clarendon Press, Oxford, 1955)
4. G. Grüner, *Density Waves in Solids* (Addison Wesley, Reading, MA, 1994)
5. A. Sacchetti, L. Degiorgi, T. Giamarchi, N. Ru, I.R. Fisher, Phys. Rev. B **74**, 125115 (2006)
6. A. Sacchetti, E. Arcangeletti, A. Perucchi, L. Baldassarre, P. Postorino, S. Lupi, N. Ru, I.R. Fisher, L. Degiorgi, Phys. Rev. Lett. **98**, 026401 (2007)
7. M. Lavagnini, A. Sacchetti, L. Degiorgi, K.Y. Shin, I.R. Fisher, Phys. Rev. B **75**, 205133 (2007)
8. K.Y. Shin, J. Laverock, Y.Q. Wu, C. Condon, M.F. Toney, S.B. Bugdale, M.J. Kramer, I.R. Fisher, Phys. Rev. B **77**, 165101 (2008)
9. F. Wooten, *Optical Properties of Solids* (Academic Press, New York, 1972)

10. M. Dressel, G. Grüner, *Electrodynamics of Solids* (Cambridge University Press, 2002)
11. T.B. Massalski, *Binary alloy phase diagrams* (ASM International, 1996)
12. E. DiMasi, B. Foran, M.C. Aronson, S. Lee, Chem. Mat. **6**, 1867 (1994)
13. J. Laverock, S.B. Dugdale, Zs. Major, M.A. Alam, N. Ru, I.R. Fisher, G. Santi, E. Bruno, Phys. Rev. B **71**, 085114 (2005)
14. Z.X. Shen, private communication
15. K.Y. Shin, V. Brouet, N. Ru, Z.X. Shen, I.R. Fisher, Phys. Rev. B **72**, 085132 (2005)
16. J.-S. Kang, C.G. Olson, Y.S. Kwon, J.H. Shim, B.I. Min, Phys. Rev. B **74**, 085115 (2006)
17. J. Laverock, S.B. Dugdale, private communication
18. In contrast to $R\text{Te}_3$ [5] and $R\text{Te}_2$ [7], two Lorentz h.o.'s are enough in $R_2\text{Te}_5$ to phenomenologically reproduce the SP mid-infrared feature defining the CDW gap. The h.o.'s mainly account for the spectral weight encountered in the SP absorption. The distribution of CDW gaps, evinced from ARPES [14,15], might also be addressed by an almost continuous distribution of Lorentz h.o.'s. Such an approach would go however beyond the scope of the Lorentz-Drude fit, because of the large amount of fit parameters thus involved.
19. M. Lavagnini, A. Sacchetti, L. Degiorgi, E. Arcangeletti, L. Baldassarre, P. Postorino, S. Lupi, A. Perucchi, K.Y. Shin, I.R. Fisher, Phys. Rev. B **77**, 165132 (2008)
20. A. Perucchi, L. Degiorgi, R.E. Thorne, Phys. Rev. B **69**, 195114 (2004)